A Novel RING-Type Ubiquitin Ligase Breast Cancer-Associated Gene 2 Correlates with Outcome in Invasive Breast Cancer

Angelika M. Burger, Yuguang Gao, Yutaka Amemiya, et al.

Cancer Res 2005;65:10401-10412.

A Novel RING-Type Ubiquitin Ligase *Breast Cancer-Associated Gene 2* Correlates with Outcome in Invasive Breast Cancer

Angelika M. Burger,[1,3] Yuguang Gao,[3] Yutaka Amemiya,[3] Harriette J. Kahn,[2] Richard Kitching,[5] Yili Yang,[6] Ping Sun,[4] Steven A. Narod,[4] Wedad M. Hanna,[2] and Arun K. Seth[1,3,5]

Laboratories of [1]Molecular Pathology and [2]Immunopathology, Department of Anatomic Pathology; [3]Division of Molecular and Cellular Biology; [4]Centre for Research in Women's Health, Sunnybrook and Women's College Health Sciences Centre; [5]Department of Laboratory Medicine and Pathobiology, Canadian Institutes of Health Research Group in Matrix Dynamics, University of Toronto, Toronto, Ontario, Canada; and [6]Regulation of Cell Growth Laboratory, Center for Cancer Research, National Cancer Institute at Frederick, NIH, Frederick, Maryland

Abstract

The RING finger family of proteins possess ubiquitin ligase activity and play pivotal roles in protein degradation and receptor-mediated endocytosis. In this study, we examined whether the *breast cancer-associated gene 2* (*BCA2*), a novel RING domain protein, has E3 ubiquitin ligase activity and investigated its expression status in breast tumors. The full-length *BCA2* gene was cloned from the human breast cancer cell line MDA-MB-468. It encodes an open reading frame of 304 amino acids and contains a RING-H2 domain. *BCA2* maps to chromosome 1q21.1, a region known to harbor cytogenetic aberrations in breast cancers. We found that the BCA2 protein has an intrinsic autoubiquitination activity, the hallmark of E3 ligases, whereas mutant RING protein is not autoubiquitinated. This indicates that the BCA2 ubiquitin ligase activity is dependent on the RING-H2 domain. Using tissue microarrays and immunohistochemistry, we found strong to intermediate BCA2 staining in 56% of 945 invasive breast cancers cases, which was significantly correlated with positive estrogen receptor status [odds ratio (OR), 1.51; $P = 0.004$], negative lymph node status (OR, 0.73; $P = 0.02$), and an increase in disease-free survival for regional recurrence (OR, 0.45; $P = 0.03$). Overexpression of BCA2 increased proliferation and small interfering RNA inhibited growth of T47D human breast cancer cells and NIH3T3 mouse cells. The autoubiquitination activity of BCA2 indicates that it is a novel RING-type E3 ligase. Its association with clinical measures and its effects on cell growth indicate that BCA2 may be important for the ubiquitin modification of proteins crucial to breast carcinogenesis and growth. (Cancer Res 2005; 65(22): 10401-12)

Introduction

RING finger proteins are implicated in human cancers and genetic disorders and play a critical role in degradation of regulatory proteins through the ubiquitin-mediated proteasome pathway (1–3). Many RING domain proteins, such as MDM2, c-Cbl, or BRCA1, have intrinsic E3 ligase activities and regulate cellular proteins that govern tumorigenesis. For example, MDM2 targets the tumor suppressor protein p53 for degradation in human cancers, whereas c-Cbl regulates cell signaling by facilitating ubiquitination and trafficking of the epidermal growth factor (EGF) receptor and the HER2 oncoproteins (4, 5). Another role is exemplified by the BRCA1 E3 ligase, which functions as a tumor suppressor involved in DNA repair and transcription (2, 4, 5).

Our laboratory has identified a novel breast cancer-associated RING domain encoding gene [*breast cancer-associated gene 2* (*BCA2*)] from among 950 cDNAs isolated by subtractive hybridization and differential display cloning techniques using normal and breast cancer cell line RNAs (6–10). We assembled a full-length open reading frame for the *BCA2* gene from expressed sequence tags before the release of the complete human genome sequence and localized it to chromosome 1q21.1 where frequent chromosomal imbalances have been reported in breast cancer (8, 11, 12). After the release of the human genome sequence, we found BCA2 to be identical to the hypothetical RING-H2 domain containing zinc finger protein 364 (ZNF364, Genbank accession no. NM_014455). The mouse homologue gene of BCA2 has been called Rabring7, a partner protein of Rab7 (13). Rab GTPases play key roles in regulating vesicle trafficking in both exocytic and endocytic pathways. As a Rab7-interacting protein, BCA2 could be recruited to specific membrane compartments by Rab7 and, thus, might be involved in the regulation of vesicle trafficking.

Here, we show that human BCA2 possesses E3 ligase activity and that autoubiquitination of BCA2 is dependent on its RING-H2 domain. We further show that BCA2 affects cell growth, if overexpressed in NIH3T3 cells or knocked down in breast cancer cells. BCA2 protein was immunohistochemically visualized using archived tumor tissue samples from the Henrietta-Banting Breast Cancer Collection (HBBCC) and patient database currently consisting of a cohort of all women who had their primary surgery for breast cancer carried out at Sunnybrook and Women's College Health Sciences Center and currently contains >2,000 cases. Statistical analyses of BCA2 protein expression results from 945 microarrayed invasive breast carcinomas show a significant correlation between overexpression of BCA2 protein and positive estrogen receptor (ER), with negative lymph node status and increased 5-year survival of regional recurrence.

Materials and Methods

Antibodies. Anti-BCA2 antibody was raised in rabbits against a synthetic pentadecapeptide sequence derived from the BCA2 COOH-terminal region conjugated to keyhole limpet hemocyanin. Rabbit IgG polyclonal antibodies were purified on a peptide affinity column. FLAG (M2) and β-actin antibodies were purchased from Sigma (St. Louis, MO). Antipolyhistidine (His-tag) antibody was from R&D Systems (Minneapolis, MN). The monoclonal antibody (mAb) antiubiquitin (P4D1) was from Cell Signaling Technologies (Beverly, MA). The mAb anti-ER (6F11) was from Novocastra (Newcastle, England). Horseradish peroxidase (HRP)–conjugated antirabbit

Requests for reprints: Arun K. Seth, Laboratory of Molecular Pathology, Department of Anatomic Pathology, Sunnybrook and Women's College Health Sciences Center, Room E423a, 2075 Bayview Avenue, Toronto, ON, Canada M4N 3M5. Phone: 416-480-6100, ext. 7974; Fax: 416-480-4375; E-mail: arun.seth@utoronto.ca.

doi:10.1158/0008-5472.CAN-05-2103

IgG and antimouse IgG secondary antibodies (Santa Cruz Biotechnology, Santa Cruz, CA) were used for Western blotting. For immunohistochemistry, EnVision Plus biotinylated antirabbit and biotinylated antimouse secondary antibodies were from DakoCytomation (Glostrup, Denmark; ref. 14).

Expression vectors and constructs. The bacterial expression vector for the E2-conjugating enzyme UbcH5b is described (15). The BCA2 cDNA was PCR amplified using open reading frame primers (5′-ATGGCGGAG-GCTTCGGCGGC-3′ and 5′-TCAGAAAGTCCATCGGTCAT-3′) from reverse-transcribed mRNAs extracted from the human breast cancer cell line MDA-MB-468. The amplicon was subcloned into the FLAG-tagged pCMV-tag2B vector (Stratagene, La Jolla, CA) and into the histidine-tagged (His6x) pET100 bacterial expression vector (Invitrogen, Carlsbad, CA). Mutations at positions cysteine 228 and 231 in the BCA2 RING domain (BCA2 amino acids 228-268: CPVCKEDYTVEEEVRQLPCNHFFHSSCIVPWLELHDTCPVC) were engineered in each wild-type (WT) construct using the Quickchange Site Directed Mutagenesis kit (Stratagene; Fig. 1*B*).

Cell culture, transfection, and immunoprecipitation. MCF7 and T47D cells were grown in RMPI 1640. HEK293T cells were maintained in high-glucose DMEM at 37°C/5% CO_2, with both media containing 10% fetal bovine serum (Sigma). For transfection experiments, 5 μg FLAG-BCA2 vector DNA were transfected into cells by the calcium chloride method and proteins were extracted 48 hours later as described previously (14). For immunoprecipitation, 1 mg of total cellular protein from transfected cells was incubated with antibody (2 μg anti-FLAG mAb, clone M2) on a shaker at 4°C for 4 hours. Similarly, 750 μg of total cellular protein from whole cell lysates of MCF7 and T47D cells were incubated with the polyclonal BCA2 antibody. Endogenous BCA2- or FLAG-BCA2–loaded beads were used for *in vitro* ubiquitination assays.

Expression of recombinant proteins. WT and mutant RING His-BCA2 were expressed in the *E. coli* strain BL21 star (DE3); expression was induced with 1 mmol/L isopropyl-1-thio-*b*-(D-galactopyranoside) for 5 hours at 37°C. BCA2 protein was purified from bacterial pellets using a Ni^{2+} chelating resin system (Probond Purification System, Invitrogen). Native buffers were used during the wash and elution steps to retain BCA2 in an undenatured state. Purified fractions were then dialyzed for 16 hours against 2 L of 50 mmol/L Tris-HCl (pH 8.0). Protein concentrations were estimated by Bradford protein assay (Bio-Rad, Hercules, CA). Crude extracts of E2-conjugating enzyme UbcH5b expressed in BL21 bacteria were used for *in vitro* ubiquitination assays as described by us earlier (15).

Ubiquitination assays. Endogenous BCA2 immunoprecipitated from T47D and MCF7 breast cancer cell lines by the polyclonal BCA2 antibody, purified recombinant His-BCA2 from bacteria, and FLAG-BCA2 immunoprecipitated from transfected HEK293T cells with anti-FLAG mAb were analyzed for E3 activity (Fig. 2). Recombinant WT and mutant His-BCA2 made in *Escherichia coli* (200 ng) were used directly, whereas Sepharose beads loaded with either BCA2/anti-BCA2 or FLAG-BCA2/anti-FLAG mAb immunoprecipitates were washed four times with TBS-T [50 mmol/L Tris-HCl (pH 8.0), 150 mmol/L NaCl, and 0.05% Triton X-100]. Bacterially expressed proteins or protein/antibody–loaded Sepharose beads were mixed with 3 μL of 20 mmol/L ATP, 1 μL ubiquitin (1 μg, Sigma), 1 μL E1 (20 ng, rabbit E1, Calbiochem, San Diego, CA), and 1 μL E2 (20 ng, UbcH5b bacterial product) in 50 mmol/L Tris-HCl (pH 8.0) were mixed with 3 μL 10× reaction buffer [500 mmol/L Tris-HCl (pH 8.0), 20 mmol/L DTT, 50 mmol/L $MgCl_2$] and 21 μL H_2O to obtain a final reaction volume of 30 μL. Each mixture was incubated at 30°C for 1 hour, then 10 μL 4× SDS gel loading buffer was added and the mixture was boiled for 3 minutes. Reactions were separated on a 4% to 20% gradient SDS-PAGE gel (Novex from Invitrogen) and subjected to immunoblotting.

Effects of zinc ejectors on BCA2 autoubiquitination. The zinc-ejecting compounds NSC667089 and disulfiram (NSC25953) were generously provided by Dr. Robert Schultz (National Cancer Institute, Developmental Therapeutics Program Central Drug Repository, Frederick, MD; refs. 16, 17). Disulfiram was chosen because it is known as a potent, but general, zinc ejector (17, 18), whereas NSC667089 very specifically inhibits the HIV type 1 nucleocapsid p7 zinc finger (16). Drug stocks (100 mmol/L) were prepared in DMSO and diluted to 100 μmol/L in 1× ubiquitination assay reaction buffer (see above). Ubiquitination assays were essentially done as described by using recombinant His-BCA2 in the presence and absence of E2-conjugating enzyme UbcH5b extract and with or without zinc-ejecting compounds. Two hundred nanograms of recombinant His-BCA2 was used with diluted drugs to obtain a final concentration of 1 or 10 μmol/L zinc ejector in 30 μL reaction volume and the mixtures were incubated at room temperature for 30 minutes before performing the ubiquitination assay.

Western blotting. Immunoprecipitates, whole cell lysates, recombinant BCA2 proteins, and *in vitro* ubiquitination mixtures were separated by SDS-PAGE electrophoresis as described elsewhere (14). Proteins were then transferred onto a Hybond P membrane (Amersham, Piscataway, NJ) and blocked overnight with 10% milk powder in TBS. The primary antibodies were added to the blocking buffer and incubated for 4 hours at room temperature (anti-FLAG 1:2,500, anti-BCA2 1:500, and antiubiquitin 1:5,000). To confirm the specificity of our polyclonal BCA2 antibody (0.45 μg/μL, 1:500), we incubated it with the BCA2 peptide used for immunization in 10-fold excess in 100 μL PBS for 30 minutes on ice before addition to the blocking buffer. Membranes were washed in TBS-Tween 20 (0.2%) and incubated with species-specific secondary antibodies

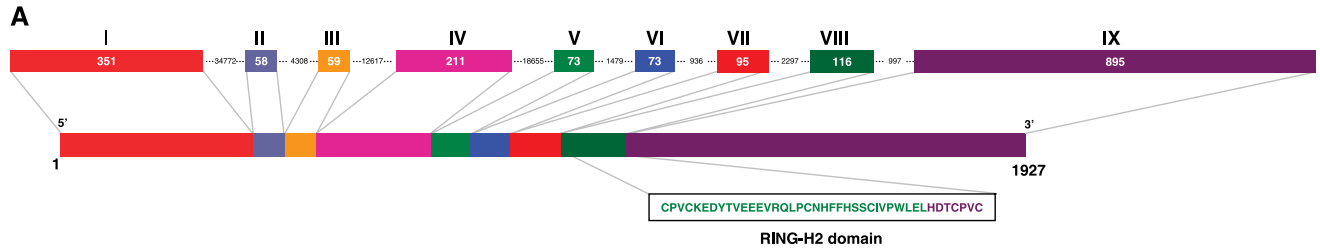

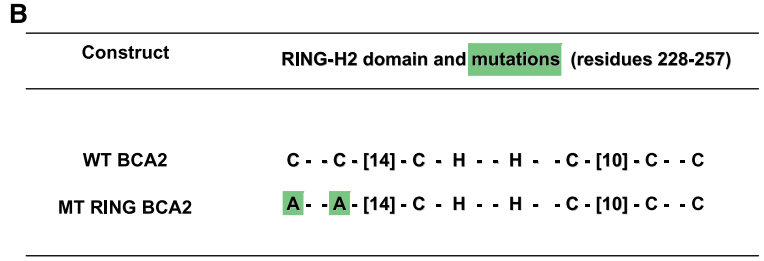

Figure 1. The *BCA2* gene. *A,* schematic diagram of the *BCA2* gene structure and mRNA. Exons are indicated by colored text: *red,* exon 1; *gray-blue,* exon 2; *orange,* exon 3; *light purple,* exon 4; *green,* exon 5; *blue,* exon 6; *dark red,* exon 7; *dark green,* exon 8; *dark purple,* exon 9. The sizes in nucleotides of each exon and intron in the genomic sequence are shown. The amino acid sequence of the RING domain is depicted with the individual amino acids colored according to their exon location. *B,* amino acid numbers and sequence of the BCA2 RING-H2 domain and mutant constructs are shown with RING mutations (*green*).

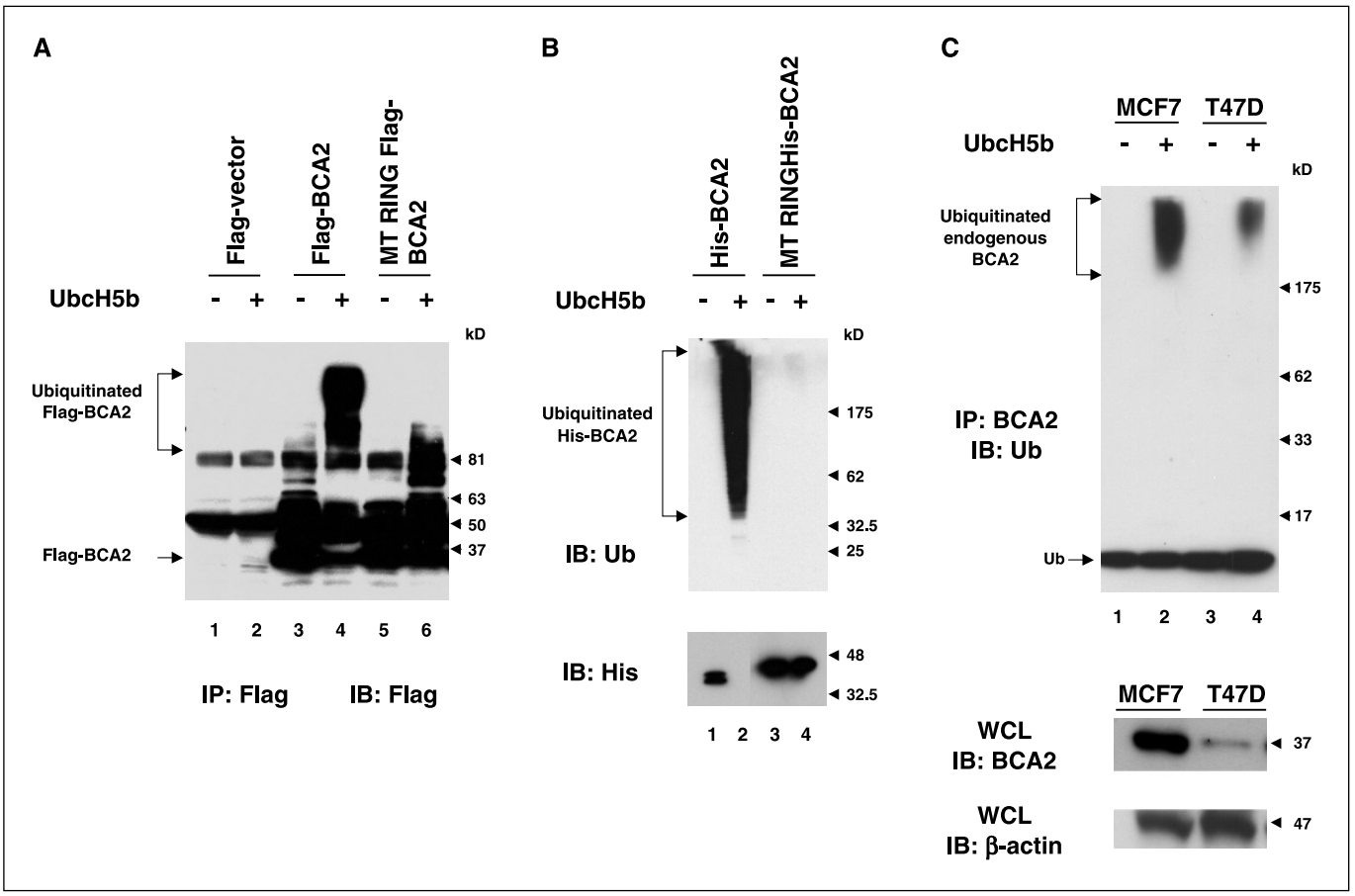

Figure 2. The BCA2 protein has autoubiquitination activity. *A,* autoubiquitination of transiently expressed BCA2 proteins: anti-FLAG immunoblot (*IB*) of proteins immunoprecipitated (*IP*) by anti-FLAG antibody from HEK293T cells transfected with the FLAG-pCMV-tg2B empty vector (*lanes 1* and *2*), FLAG, and BCA2 vector (*lanes 3* and *4*), or the FLAG-BCA2 RING mutant (*MT*; *lanes 5* and *6*) and incubated with (*even lanes*) or without (*odd lanes*) the bacterial extract containing UbcH5b E2 ubiquitin-conjugating enzyme, purified ubiquitin (Sigma), and E1 protein (Calbiochem). *B,* autoubiquitination of recombinant BCA2 protein: antiubiquitin (*top*) and anti-His (*bottom*) immunoblots of *in vitro* ubiquitination reactions using bacterially expressed His-BCA2 (*lanes 1* and *2*) or His-BCA2 RING domain mutant (*lanes 3* and *4*) in the presence (*even lanes*) or absence (*odd lanes*) of bacterial extract containing the E2-conjugating enzyme UbcH5b and purified ubiquitin with E1 protein. *C,* autoubiquitination of endogenous BCA2 protein: BCA2 protein was immunoprecipitated (*top*) by the anti-BCA2 antibody from whole cell lysates of MCF7 or T47D breast cancer cell lines and then incubated with (*even lanes*) or without (*odd lanes*) recombinant UbcH5b, ubiquitin, and the E1 protein. Ubiquitination of BCA2 was detected using antiubiquitin antibodies (*top*). Immunoblots for anti-BCA2 (*middle*) and antiactin (*bottom*) in whole cell lysate (*WCL*) of MCF7 or T47D cells are indicated.

conjugated to HRP for 1 hour. Signals were developed by using an enhanced chemiluminescence kit (Amersham) and by exposure to X-ray film (Kodak, Rochester, NY).

Analysis of BCA2 protein stability. To determine the stability of endogenous BCA2, 1×10^6 MCF7 cells were seeded into six-well plates and grown overnight. The protein synthesis inhibitor cyclohexamide (Sigma) was added alone (100 μmol/L) or in combination with the proteasome inhibitor MG-132 (10 μmol/L, Calbiochem) for a total of 1 and 8 hours. Control cells were treated with combined vehicle (DMSO and ethanol) for 1 and 8 hours. To examine whether the BCA2 stability is linked to autoubiquitination, WT and mutant RING BCA2 were exogenously expressed in HEK293T cells. Five micrograms of WT or mutant RING FLAG-BCA2 vector DNA were transfected as described above. After 24 hours, the protein synthesis inhibitor cycloheximide (Sigma) was added alone (100 μmol/L) or in combination with the proteasome inhibitor MG-132 (10 μmol/L) for a total of 1, 6, or 24 hours. Control cells were treated with vehicle (DMSO and/or ethanol) for 24 hours. Whole cell lysates were analyzed for protein expression by Western blotting.

BCA2 knockdown by small interfering RNA. Custom-designed small interfering RNA (siRNA) duplexes were purchased from Qiagen [BCA2 siRNA duplex 1, sense r(GGCUGUGGUAAUCAUCUUA)dTdT, antisense r(UAAGAUGAUUACCACAGCC)dCdT; BCA2 siRNA duplex 2, sense r(CGUCUGAAUAGAAUUAAUU)dTdT, antisense r(AAUUAAUUCUAUUCAGACG)dGdG; HiPerformance 2-for-Silencing, Qiagen, Valencia, CA] and dissolved in siRNA suspension buffer to yield a stock of 20 μmol/L. Nonsilencing control siRNA (RNAi human/mouse control kit; Qiagen) was used as negative control and RNAiFect (Qiagen) was used as a transfection reagent.

Proliferation and invasion assay. pCMV-tg2B vector containing the FLAG-BCA2 insert was transfected into the NIH3T3 cells and cloned using G418 selection and the dilution method. Clone 5 produced high levels of BCA2 and was further investigated. To study the growth of the stable NIH3T3 FLAG-BCA2-clone 5 cell line compared with parental NIH3T3 cells, 100, 500, and 1,000 cells were seeded in 96-well plates (n = 12 wells) and grown for 6 days followed by the 3-(4,5-dimethylthiazol-2-yl)-2,5-diphenyltetrazolium bromide (MTT) assay (19). Effects of BCA2 siRNA duplex 2 on growth were determined in T47D breast cancer cells seeded in 96-well plates at a density of 2,000 cells per well. MCF-7 cells were used to study BCA2 effects on invasive growth using six-well plates with Transwell inserts; 200,000 cells were seeded into each insert in medium containing BCA2 siRNA, as well as siRNA suspension buffer and RNAiFect transfection reagent that were used as negative controls. Growth of cells in 96-well plates and cells that had migrated from the Transwell into the bottom chamber of six-well plates was evaluated by MTT assay after 6 days of continuous exposure to treatments. Reduction of MTT by vital cells into insoluble formazan was measured at 540 nm after the purple formazan crystals were

dissolved in DMSO using a PowerWaveX340-I plate reader and KC4 software (Bio-Tek, Winooski, VT).

Northern blotting. Normal human tissue blots were purchased from Clontech (BD Biosciences MTN, Palo Alto, CA). Northern blot membranes of human tumor cell lines and NIH3T3 mouse fibroblast clones were generated by us, and BCA2 probe labeling and hybridization procedures were done as reported previously using the human BCA2 cDNA as template (6, 7).

The Henrietta-Banting Breast Cancer Collection and patient database. The HBBCC consists of paraffin blocks from 1,800 invasive breast cancers from patients that presented at Women's College and Sunnybrook Hospitals in Toronto, Ontario, Canada, between 1987 and 1997. Patients have been followed for 5 to 17 years. We created the accompanying database from information abstracted from the hospital and provincial patient records. The HBBCC database includes tumor grade, demographic variables, treatments, and outcomes as listed in Table 1.

Tissue microarrays. Breast tissue microarrays were assembled and transferred onto slides following the tissue microarray method as described earlier (14, 20). In brief, formalin-fixed, paraffin-embedded breast tumor specimens and their corresponding H&E-stained slides were selected from the HBBCC. Tissues were anonymized by stripping all identifiers from each case. Areas of cancer and normal tissue were marked on H&E sections for core biopsy by pathologists (H.J. Kahn and W. Hanna). One thousand and forty-six of 1,800 invasive breast cancer cases had sufficient tumor material to be included in the microarrays and a total of 945 informative cases were available. Eleven breast tumor tissue arrayed blocks containing 300 cores per block were constructed with each case represented by three separate cores (100 cases in triplicate per slide).

Immunohistochemistry. Tissue microarrays were sectioned and dewaxed. Antigen retrieval was done by heating the slides in a microwave oven for 20 minutes in citrate buffer (pH 6.0). Tissue microarray slides were incubated with BCA2 antibody (0.45 mg/mL, 1:100 dilution) overnight followed by an incubation with biotinylated antirabbit antibody for 2 hours. Negative controls were BCA2 antibody preincubated with excess BCA2 peptide for 30 minutes before the primary antibody incubation as well as slides processed without primary antibody. The anti-ER mAb was diluted and used according to the instructions of the manufacturer. Biotinylated secondary antibodies were visualized using the Envision plus kit (DAKOCytomation, Glostrup, Denmark) and diaminobenzidine was used as substrate. Slides were then counterstained with hematoxylin, dehydrated, and cleared. Immunostaining and clinicopathologic features were evaluated microscopically by two pathologists (H.J. Kahn and W. Hanna).

Table 1. Comparison of groups for clinicopathologic variables of 945 patients

Variables	BCA2 ≤ 1, *N* = 415 (43.9%)	BCA2 > 1, *N* = 530 (56.1%)	*P**
Mean age of diagnosis (range)	55.6 (22.9-93.4)	57.0 (24.5-91.5)	0.13
Node status, *n* (%)			
Negative	156 (42.2)	230 (50.1)	0.02
Positive	213 (57.7)	229 (49.9)	
NE	46	71	
BR grade (%)			
1	54 (16.7)	54 (12.7)	0.16
2	138 (42.6)	207 (48.1)	
3	132 (40.7)	164 (38.6)	
NE	91	105	
LVI, *n* (%)			
No	226 (62.6)	305 (64.1)	0.66
Yes	135 (37.4)	171 (35.9)	
NE	54	54	
ER, *n* (%)			
Negative ≤ 10%	144 (35.3)	134 (26.5)	0.004
Positive >10%	264 (64.7)	371 (73.5)	
NE	7	25	
Tumor size (mm)	26.6 (1-220)	25.2 (1-105)	0.22
NE	10	8	
Histology, *n* (%)			
DUC	315 (75.9)	391 (73.7)	0.30
LOB	33 (8.0)	58 (10.9)	
Other	67 (16.1)	81 (15.3)	
TAM, *n* (%)			
No	188 (46.1)	248 (47.9)	0.59
Yes	220 (53.9)	270 (52.1)	
NE	7	12	
Chemo, *n* (%)			
No	262 (64.4)	348 (66.4)	0.52
Yes	145 (35.6)	176 (33.6)	
NE	8	6	

Abbreviations: BR, Bloom Richardson grade; LVI, lymph invasion; DUC, invasive ductal carcinoma; LOB, invasive lobular carcinoma; TAM, tamoxifen treatment; Chemo, chemotherapy; NE, not evaluable.
*Student's *t* test was used to compare means; χ^2 test was used to compare frequency; missing values were not included in all the tests.

Table 2. Cox proportional hazard regression analyses on the relative risk of variables in 5-year survival of recurrences/death in the HBBCC

Recurrence	Univariate		Multivariate*	
	RR (95% CI)	*P*	RR (95% CI)	*P*
Local				
BCA2	0.79 (0.51-1.20)	0.26	0.94 (0.57-1.55)	0.81
Age at diagnosis	0.98 (0.96-1.00)	0.02	1.00 (0.98-1.02)	0.70
Tumor size	1.02 (1.01-1.03)	0.001	1.01 (1.00-1.03)	0.02
BR grade (trend)	1.85 (1.25-2.75)	0.002	1.50 (1.00-2.26)	0.05
BR grade 2 vs 1	1.52 (0.58-3.49)	0.39	1.47 (0.56-3.87)	0.44
BR grade 3 vs 1	3.03 (1.19-7.73)	0.02	2.23 (0.85-5.82)	0.10
ER	0.52 (0.34-0.81)	0.003	0.59 (0.34-0.99)	0.05
Regional				
BCA2	0.52 (0.30-0.91)	0.02	0.45 (0.22-0.91)	0.03
Age at diagnosis	0.99 (0.97-1.01)	0.17	1.00 (0.97-1.03)	0.96
Tumor size	1.01 (1.00-1.02)	0.01	1.01 (0.99-1.02)	0.31
BR grade (trend)	3.50 (1.84-6.66)	<0.0001	2.68 (1.39-5.14)	0.003
BR grade 2 vs 1	0.52 (0.12-2.18)	0.37	0.56 (0.13-2.35)	0.43
BR grade 3 vs 1	3.69 (1.12-12.1)	0.03	2.90 (0.86-9.80)	0.09
ER	0.26 (0.15-0.46)	<0.0001	0.44 (0.21-0.90)	0.03
Distant				
BCA2	0.84 (0.63-1.13)	0.26	0.90 (0.62-1.30)	0.57
Age at diagnosis	0.97 (0.95-0.98)	<0.0001	0.98 (0.97-1.00)	0.007
Tumor size	1.02 (1.02-1.03)	<0.0001	1.01 (1.01-1.02)	<0.0001
BR grade (trend)	3.10 (2.23-4.31)	<0.0001	2.28 (1.62-3.21)	<0.0001
BR grade 2 vs 1	6.20 (1.49-25.2)	0.01	6.04 (1.46-25.0)	0.01
BR grade 3 vs 1	17.2 (4.20-69.7)	<0.0001	11.4 (2.78-46.8)	0.007
ER	0.38 (0.28-0.51)	<0.0001	0.65 (0.44-0.96)	0.03
Death				
BCA2	0.90 (0.66-1.22)	0.50	0.98 (0.67-1.45)	0.93
Age at diagnosis	1.00 (0.99-1.01)	0.74	1.01 (1.00-1.03)	0.07
Tumor size	1.02 (1.02-1.03)	<0.0001	1.02 (1.01-1.02)	<0.0001
BR grade (trend)	2.44 (1.77-3.37)	<0.0001	1.94 (1.38-2.72)	<0.0001
BR grade 2 vs 1	1.82 (0.76-4.34)	0.18	2.07 (0.81-5.28)	0.13
BR grade 3 vs 1	4.82 (2.10-11.1)	0.002	3.93 (1.57-9.86)	0.004
ER	0.34 (0.27-0.50)	<0.0001	0.52 (0.56-0.78)	0.002

NOTE: The relative risk of age at diagnosis is the risk of every patient 1 year older at diagnosis. For BCA2, it is the risk of BCA2 > 1 (BCA2 ≤ 1 is the baseline); for ER, it is the risk of ER > 10% (ER ≤ 10% used as baseline); for tumor size, it is the risk for every 1 mm increase of the tumor size; for BR grade trend, it is the risk of every BR grade increase; for BR grade 2 versus 1 (or 3 versus 1), the BR grade 1 was used as baseline.
Abbreviations: RR, relative risk; 95% CI, 95% confidence interval.
*The model was run thrice to get the relative risks of Bloom Richardson grade trend, Bloom Richardson grade 2 versus 1, and Bloom Richardson grade 3 versus 1.

Immunohistochemical scoring system. ER expression was scored according to established procedures for immunohistochemical staining (21). Cases with <10% positive cells were considered negative; cases with >10% stained cells were considered positive. BCA2 staining was evaluated using an established method (14, 22) as follows: 0, no expression; 1, weak expression; 2, moderate expression; 3, strong to very strong expression (Fig. 6). For statistical analysis, the HBBCC cases were divided into two groups: tumors expressing BCA2 of 0 to 1 (BCA2 <1) or >1 (BCA2 < 1). All BCA2-positive cases showed staining in >90% of invasive cancer cells (14, 22).

Statistical analysis. BCA2 expression was correlated with demographic data, pathologic variables, and treatment modalities. The list of variables includes age, node status, grade, lymphovascular invasion, ER status, tumor size, histology, tamoxifen treatment, and chemotherapy (listed in Tables 1-3). Statistical analyses were carried out using Fischer's exact test or *t* test to compare means and the χ^2 test to compare frequency distributions. All statistical tests were two-sided. Multivariate and univariate survival analyses were based on Cox proportional hazard regression analyses and used to assess the relative risks of recurrence and of death among patients who did, and who did not, overexpress BCA2 (Tables 2 and 3). Five-year survival curves were constructed according to the Kaplan-Meier method and were compared using the log-rank test. $P < 0.05$ was considered to be statistically significant. The odds ratio (OR) was calculated according to the Cochrane definition. The SAS 8.2 software package (ITS, Austin, TX) was used for analysis.

Results

The *BCA2* gene. The *BCA2* gene was initially identified as a 325 bp partial cDNA sequence (termed T3A12) cloned from a subtractive hybridization library derived from matched breast tumor and normal breast cell line mRNAs (7). At the time of

Table 3. Overall survival of cancer reoccurrence and death in patients with BCA2 ≤ 1 or BCA2 > 1

Variables	BCA2 ≤ 1, *N* = 415 (43.9%)	BCA2 > 1, *N* = 530 (56.1%)	*P**
Followed-up, y (SD)	7.4 (3.5)	6.8 (3.2)	0.01
Range	0.05-16.3	0.02-16.4	
Local recurrence, *n* (%)			
Yes	51 (12.5)	55 (10.4)	
No	358 (87.5)	472 (89.6)	0.33
Mean (range)†	3.5 (0.13-14.1)	3.0 (0.13-7.8)	0.36
Regional recurrence, *n* (%)			
Yes	35 (8.6)	28 (5.3)	
No	372 (91.4)	498 (94.7)	0.05
Mean (range)†	2.9 (0.13-10.8)	3.5 (0.16-9.0)	0.37
Distant recurrence, *n* (%)			
Yes	115 (28.2)	122 (23.3)	
No	293 (71.8)	402 (76.7)	0.09
Mean (range)†	3.5 (0.1-13.3)	3.6 (0.4-14.7)	0.84
Death, *n* (%)			
Dead	127 (30.6)	152 (28.7)	
Alive	288 (69.4)	378 (71.3)	0.52
Mean (range)†	4.8 (0.7-14.2)	4.8 (0.3-15.1)	0.99

NOTE: Missing data are not included in the analyses.
*Student's *t* test was used to compare means of groups; χ^2 test was used to compare the frequencies.
†Mean period from the first surgery (before the recurrence) to the date of recurrence/death and is only for patients who had recurrence or are dead.

cloning, this cDNA had no identity to any known gene, and we subsequently deposited it as Genbank accession no. AW225336. We extended the original cDNA sequence of *BCA2* to 1,927 bp by comparison with expressed sequence tags and cloned the open reading frame by reverse transcription-PCR. After release of the human genome, we found that *BCA2* is identical to the hypothetical zinc finger protein ZNF364 (accession no. NM_014455). By comparison with human genome contigs, we found that the *BCA2* gene contains nine exons located between nucleotides 796,131 and 874,154 of *Homo sapiens* chromosome 1 genomic contig Hs1_4591 (NT_004434; Fig. 1*A*). The predicted 304-amino-acid sequence encoded by the BCA2 open reading frame contains a RING-H2 finger domain, a feature of E3 ligases that have roles in ubiquitin-mediated trafficking and proteasome-mediated protein destruction (Fig. 1*A*).

BCA2 has E3 ubiquitin ligase activity. Autoubiquitination and ubiquitination of target proteins have been described as general functions of most of the RING domain–containing proteins (1, 15, 23, 24). We discovered that epitope-tagged BCA2 (Fig. 2*A*), as well as recombinant (Fig. 2*B*) and endogenous BCA2 from MCF7 and T47D breast cancer cell lines (Fig. 2*C*), have intrinsic autoubiquitination activity. BCA2 from all three sources is auto-ubiquitinated only in the presence of E2 ubiquitin–conjugating enzyme UbcH5b (Fig. 2*A-C*), whereas a mutant BCA2 with a disrupted RING domain was not ubiquitinated even in the presence of the UbcH5b E2 (Fig. 2*B*). In addition to mutation inactivation, we were able to inhibit BCA2 autoubiquitination activity by including the broad-spectrum, zinc-ejecting compound disulfiram, but not by the HIV type 1 nucleocapsid p7 zinc finger–specific drug NSC667089 in the *in vitro* ubiquitination reactions (Fig. 3; refs. 16, 17).

BCA2 is stabilized by inhibition of the proteasome. To examine the stability of endogenous BCA2, we used the breast cancer cell line MCF7, which expresses high levels of BCA2. When protein synthesis was inhibited by treatment with cyclohexamide alone, a marked decline of BCA2 expression was seen after 8 hours (Fig. 4*A, lane 3*) and this degradation of BCA2 was reduced by treatment with the proteasome inhibitor MG-132 (Fig. 4*A, lanes 4* and *5*). Whether BCA2 stability is related to autoubiquitination

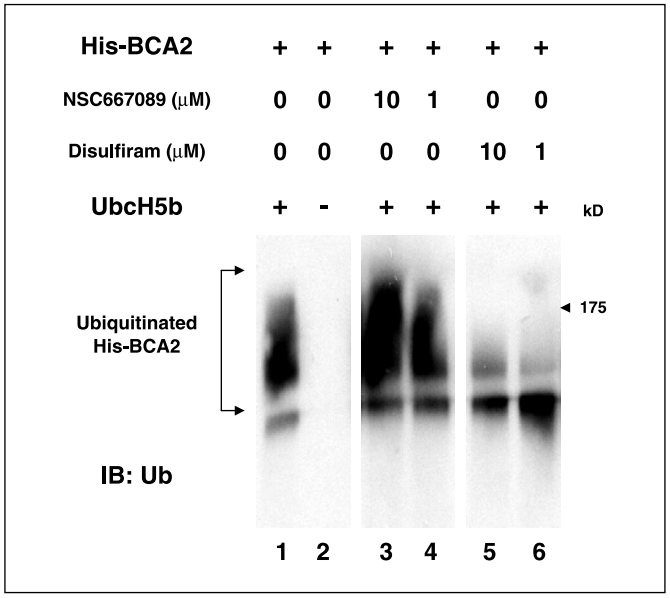

Figure 3. BCA2 autoubiquitination activity can be inhibited by zinc-ejecting compounds. An antiubiquitin immunoblot of *in vitro* ubiquitination reactions containing ubiquitin, bacterially expressed His-BCA2, UbcH5b-conjugating enzyme (*lanes 1* and *3-6*), and one of the zinc-ejecting compounds NSC667089 (*lanes 3* and *4*) or disulfiram (*lanes 5* and *6*).

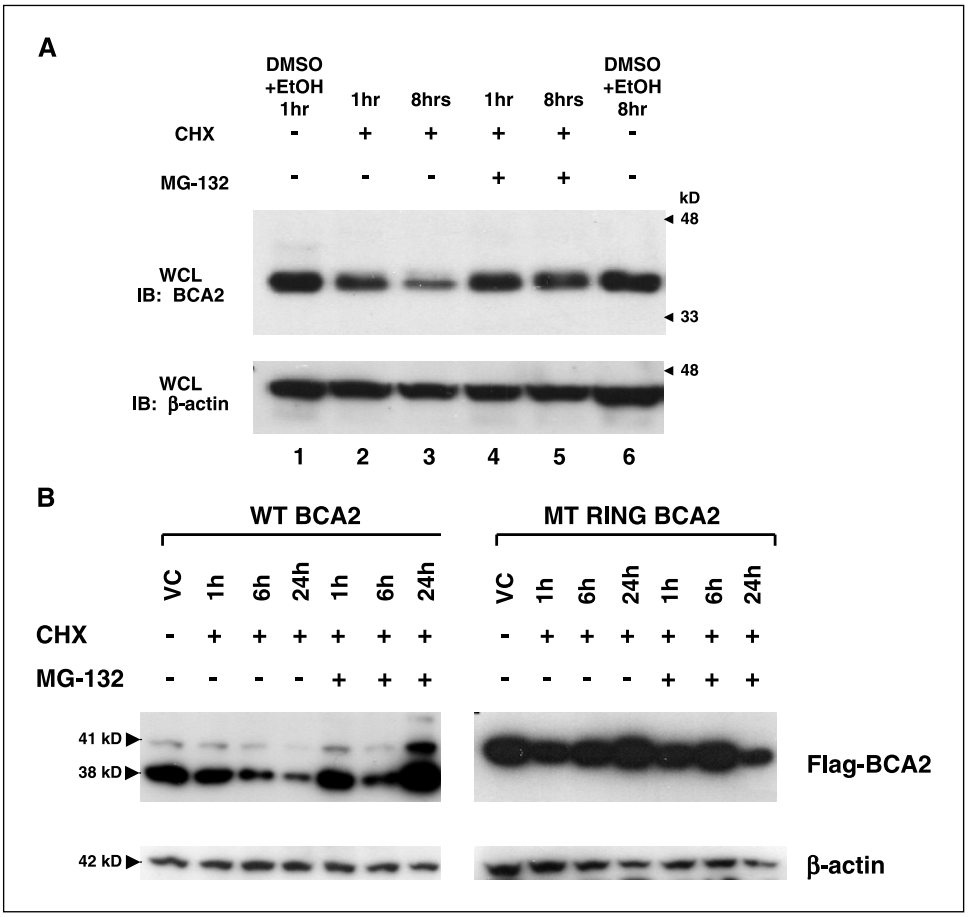

Figure 4. *A,* endogenous BCA2 can be stabilized by proteasome inhibition. Anti-BCA2 (*top*) immunoblot and reblot with antiactin (*bottom*) containing proteins from whole cell lysates of MCF7 breast cancer cells treated with the protein synthesis inhibitor cyclohexamide (*CHX*; *lanes 2-5*) in the presence (*lanes 4* and *5*) and absence (*lanes 1-3* and *6*) of the proteasome inhibitor MG-132 for 1 or 8 hours as indicated. BCA2 expression in vehicle control cells was determined using DMSO and ethanol without drugs for 1 hour (*lane 1*) or 8 hours (*lane 6*). *B,* stability of WT BCA2 versus the RING mutant. Equal amounts of WT BCA2 or mutant RING BCA2 vector DNA was transfected into HEK293T cells. The total transfection period was 48 hours. Cycloheximide (100 μmol/L) was added 24, 42, and 47 hours (*h*) after transfection, either alone or together with MG-132 (10 μmol/L), resulting in drug exposure of 1, 6, or 24 hours. Vehicle controls (*VC*) were 24 hours treated with ethanol and DMSO. β-actin was used as a loading control.

was evaluated by transfecting WT FLAG-BCA2 and mutant FLAG-RING BCA2 into HEK293T cells (Fig. 4*B*). We observed higher levels of exogenous mutant RING BCA2 protein in whole cell lysates compared with WT BCA2 (Fig. 4*B*). When protein synthesis was inhibited by treatment with cycloheximide, a decline after 6 hours was seen for WT, but not for mutant RING protein levels. Moreover, whereas WT BCA2 protein could be stabilized with the proteasome inhibitor MG-132, mutant RING protein levels were not affected (Fig. 4*B*). WT BCA2 showed a half-life of 6 hours, whereas mutant RING BCA2 seems to be stable for >24 hours (Fig. 4*B*). WT BCA2 runs as a doublet and the mutant protein with a disrupted RING domain runs as the larger of the two bands, suggesting a conformational change of the protein structure after mutation of the Zn^{2+}-complexing cysteine residues.

BCA2 expression in normal and tumor cells. BCA2 RNA is expressed at extremely low levels in normal tissues, such as breast, prostate, lung, and colon; however, heart, skeletal muscle, and testis showed moderate expression (Fig. 5*A*). In contrast, much higher BCA2 levels are seen in breast and prostate cancer cell lines with the ER-positive cell line MCF7 having the highest BCA2 RNA expression (Fig. 5*B*). Three distinct bands were detected in heart and skeletal muscle tissues; two bands were detected in the breast and prostate cancer cells. Different BCA2-specific bands could represent alternative 5′ or 3′ untranslated regions, differential splicing, or polyadenylic acid signals.

BCA2 protein expression was examined by immunoblotting of whole cell lysates from the T47D breast cancer cell line. Endogenous BCA2 yielded a specific signal of 37 kDa (Fig. 5*C*) using our polyclonal rabbit BCA2 antibody as a primary antibody. Confirmation of antibody specificity was shown by prior incubation of the BCA2 antibody with the specific BCA2 immunizing peptide, which resulted in blockage of the BCA2 signal in T47D lysates (Fig. 5*C, right*). Invasive breast cancer tissues were also positive for BCA2 protein with our antibody, and, again, preincubation with the specific immunizing peptide blocked the immunohistochemical signal (Fig. 5*D, right*). BCA2 siRNA knockdown experiments using the MCF7 cell line resulted in a clear reduction of the endogenous BCA2 band compared with control siRNA (Fig. 5*E*). However, BCA2 siRNA duplex 1 was less effective than siRNA duplex 2; subsequently, only BCA2 siRNA duplex 2 was used for the growth assays described below.

BCA2 expression in breast cancer tissue microarrays. Nine hundred and forty-five invasive breast carcinomas of the HBBCC were stained and evaluated for BCA2 and ER expression. Representative core samples are shown in Figs. 5-7. Four hundred and fifteen cases (43.9%) had low nuclear BCA2 levels (BCA2 ≤ 1; Fig. 7). Five hundred and thirty patient tissues (56.1%) were found to overexpress BCA2 in nucleus and cytoplasm (BCA2 > 1; Fig. 6*C* and *D*; Table 1). Normal breast tissues also expressed low amounts of BCA2 protein (Fig. 6*A*). Seventy percent (635) of invasive breast cancers were ER positive (Table 1; Fig. 7).

Statistical significance of clinicopathologic variables in the Henrietta-Banting Breast Cancer Collection. Univariate and multivariate proportional hazard Cox regression analyses revealed that for the invasive breast cancers of the HBBCC, tumor size

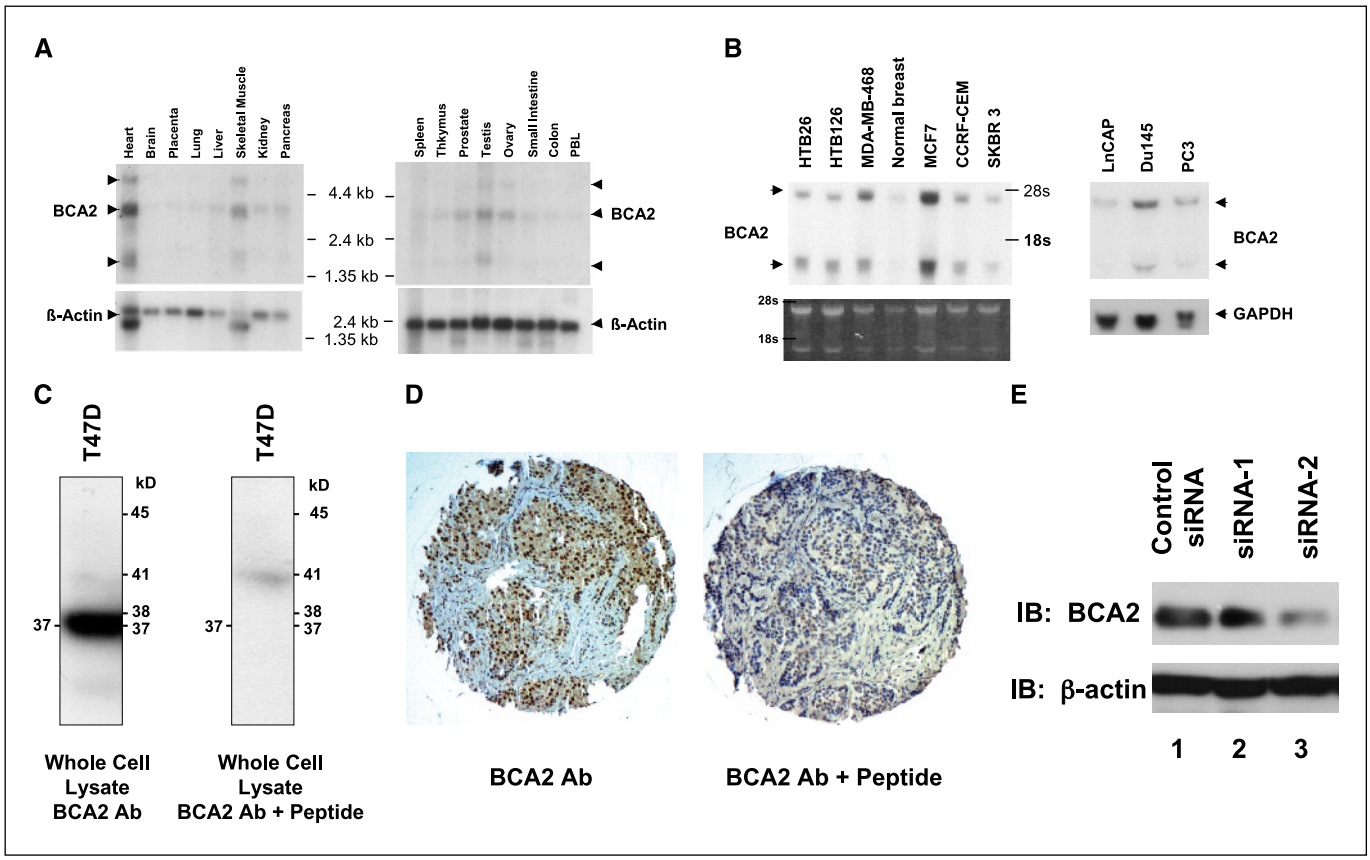

Figure 5. Multiple tissue Northern blots and BCA2 antibody specificity. *A,* autoradiogram of Northern blot of total RNA from human normal tissues (Clontech) after hybridization with cDNA probes for BCA2 (*top*) or β-actin (*bottom*). *B,* autoradiogram of Northern blot of total RNA from the indicated tumor cell lines and normal breast cells after hybridization with cDNA probes for BCA2 (*top*) or glyceraldehyde-3-phosphate dehydrogenase (*GAPDH*; *bottom, right*) as well as photograph of ethidium bromide fluorescent RNA of the agarose gel (*bottom, left*). *C,* anti-BCA2 immunoblots of T47D whole cell lysates done without (*left*) or with (*right*) the peptide used to generate the polyclonal BCA2 antibody. *D,* peroxidase/3,3′-diaminobenzidine immunostaining of invasive breast cancer cells using the BCA2 antibody (*Ab*) in the absence (*left*) or presence (*right*) of the peptide used to generate the polyclonal BCA2 antibody. *E,* anti-BCA2 (*top*) and antiactin immunoblots of whole cell lysates from MCF7 cells treated with a nonsilencing control siRNA duplex (*lane 1*), BCA2 siRNA 1 (*lane 2*), or BCA2 siRNA duplex 2 (*lane 3*).

($P < 0.0001$), tumor grade ($P < 0.0001$), and ER status ($P < 0.002$) were significant predictors of death within 5 years of diagnosis (Table 2). Distant metastases correlated with age at diagnosis ($P = 0.007$), tumor size ($P < 0.0001$), tumor grade ($P < 0.0001$), and ER ($P = 0.03$), whereas regional recurrences were related to tumor grade ($P = 0.003$) and ER ($P = 0.03$). Moreover, local recurrences were related to tumor size, grade, and ER status (Table 2). Our results indicate that the HBBCC reflects the standard behavior of invasive breast cancers and that the prognostic indicators are represented.

BCA2 levels correlate with regional recurrence and lymph node metastasis. We tested the effects of BCA2 expression levels on mean age at diagnosis, node status, Bloom Richardson grade, lymphatic invasion, ER, tumor size, histology (Table 1), as well as local, regional, or distant recurrences and death (Table 3). Three variables yielded statistically significant results when correlated with BCA2 expression: (*a*) Patients with BCA2 ≤ 1 (43.9% of the group) were more likely to have lymph node metastasis at presentation than those with BCA2 > 1 (56.1% of the group, $P = 0.02$; Table 1). (*b*) Women with invasive breast cancers with BCA2 ≤ 1 were more likely to experience regional reoccurrence than those with BCA2 > 1 (OR, 0.45, $P = 0.05$; Table 3; and $P = 0.02$ log-rank adjusted for time from diagnosis to recurrence; Fig. 8). Moreover, univariate and multivariate Cox regression analyses yielded significance for BCA2 overexpression in the 5-year disease-free survival for regional recurrences (Table 2). A similar trend was seen for overall distant metastasis, but not for local occurrence (Table 3). (*c*) Nuclear BCA2 correlated with positive ER status (Table 1; Fig. 8). Of the 945 invasive HBBCC cases, 67.1% were ER positive and 83% of those were also BCA2 positive ($P = 0.004$, Table 1).

BCA2 and estrogen receptor are coexpressed. Because of the significant statistical correlation found between invasive breast cancers expressing ER and BCA2 (Table 1), we compared the pattern of expression of these two proteins. Core by core analysis indicates that BCA2 and ER are mostly coexpressed (OR, 1.5). As represented by cases shown in Fig. 7, cells strongly positive for BCA2 were positive for ER, with BCA2 and ER predominantly found in the nucleus of breast cancer tissues. These findings suggest that BCA2 is highly expressed in ER-positive tumors.

BCA2 affects breast cancer cell growth. To investigate whether BCA2 plays role in cell proliferation, we transfected NIH3T3 cells with the human full-length *BCA2* cDNA (pCMV-tag2B-BCA2). The growth of NIH3T3 BCA2-FLAG clone 5, which expresses high levels of BCA2 at the RNA and protein level (Fig. 9*A*), was compared with the growth of its parental line ($P = 0.02$ and 0.01, respectively; Fig. 9*B*). The MTT proliferation assay indicates that BCA2 expression caused a 50% increase in the

proliferative capacity of NIH3T3 cells (Fig. 9*B*). In contrast, treatment of T47D breast cancer cells with BCA2 siRNA duplex 2 produced a marked reduction of growth at concentrations of 100 and 20 nmol/L ($P = 0.02$; Fig. 9*C*). Moreover, MCF-7 cells grown in the presence of 100 nmol/L BCA2 siRNA duplex 2 had a decreased ability to grow through Transwell membranes (25, 26) which is indicative of inhibition of their invasive growth behavior (Fig. 9*D*). MCF-7 cells treated with vehicle control (siRNA suspension buffer) or with RNAifect were compared. MCF-7 cells treated with 100 nmol/L BCA2 siRNA duplex 2 showed a decrease in motility of 31%, which is statistically significant ($P = 0.001$).

Discussion

The RING domains of RING-type E3 ligases bind the E2 ubiquitin-conjugating enzymes complexes via cysteine/histidine residues that form a zinc ion–stabilized cross-brace structure (2). As part of our integrated study of the human breast cancer genome anatomy, we discovered that the *BCA2* gene encodes a RING-H2 domain (Fig. 1). The protein sequence is conserved in various species (mouse, fruit fly, and fission yeast; data not shown), suggesting important function(s) for this E3 ubiquitin ligase. The role of RING domains lies generally in the realm of protein-protein interactions and ubiquitination and Fig. 2*A-C* clearly shows that BCA2 exhibits the E3 ligase activity (1–3). Endogenous, exogenous, and recombinant BCA2 proteins were capable of polyubiquitinating themselves in the presence of an E1- and E2-conjugating enzyme, but not in the absence of an E2-conjugating enzyme. In addition, autoubiquitination was abolished by mutation of two essential cysteine residues to alanines in the RING domain and by withdrawal of zinc by the potent zinc-ejecting compound disulfiram (Fig. 3).

Disulfiram, a drug marketed as an alcohol dehydrogenase inhibitor (Antabuse), is also known for its zinc-ejecting properties (17, 18). Most recently, disulfiram was described to inhibit angiogenesis and invasion of human tumor and umbilical vein endothelial cells owing to their dependence on zinc chelating proteins. Several zinc-ejecting agents (18), such as NSC667089, have been shown to very specifically target zinc and RING finger proteins, including E3 ligases (6, 16, 17). Hence, it is possible that disulfiram analogues could be developed, which specifically modulate BCA2 activity and provide a novel approach for the treatment of breast cancer.

The involvement of BCA2 in the ubiquitin-proteasome system based on its RING finger domain is further reflected in the protein stability experiments. When overall protein synthesis was inhibited by cycloheximide, endogenously and exogenously expressed BCA2 were gradually degraded (Fig. 4*A* and *B*). When the proteasome inhibitor MG-132 was added together with cyclohexamide, BCA2 degradation was significantly reduced or prevented. Moreover, the RING mutant BCA2 was resistant against degradation and proteasome inhibition, suggesting that effects seen on WT BCA2 are related to its ubiquitination. Similar resistance to proteasome-mediated degradation has been reported previously for the IAP-1 RING mutant E3 ligase, resulting in relative higher protein levels compared with WT IAP-1 (15).

Among the peptide growth factors active in breast glandular cell proliferation, EGF is thought to play a key role in tumor development, growth, and invasion, and EGF receptor is overexpressed in human breast cancer cells (27, 28). BCA2 has been shown to be recruited to the late endosome/lysosome by the GTP-bound form of Rab7, which causes a perinuclear aggregation

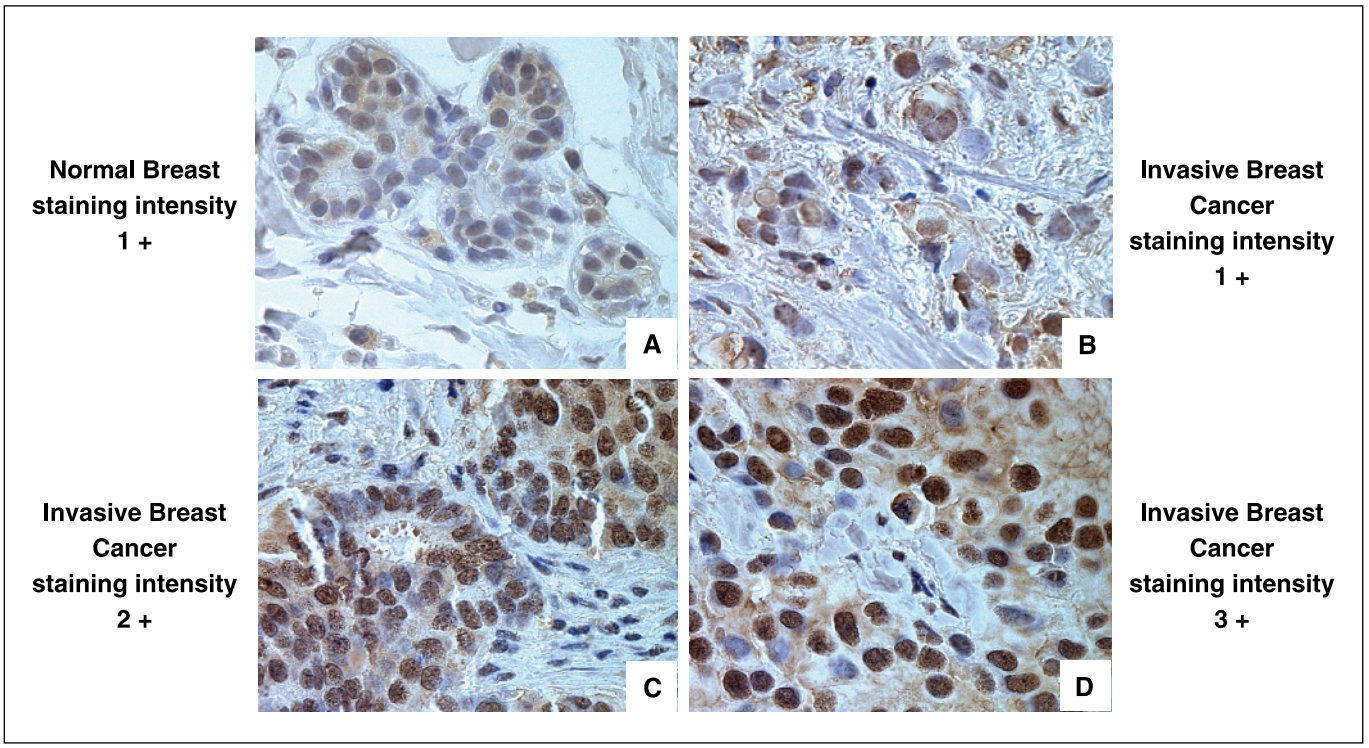

Figure 6. Representative microarrayed tissue sections demonstrating the scoring system used to rank BCA2 expression in 945 invasive breast tumors. *A,* normal breast tissue with weak (1+) nuclear and cytoplasmic BCA2 staining intensity. *B,* invasive breast cancer with weak (1+) BCA2 staining intensity. *C,* invasive breast cancer with moderate (2+) BCA2 intensity. *D,* invasive breast tumor with strong (3+) BCA2 intensity.

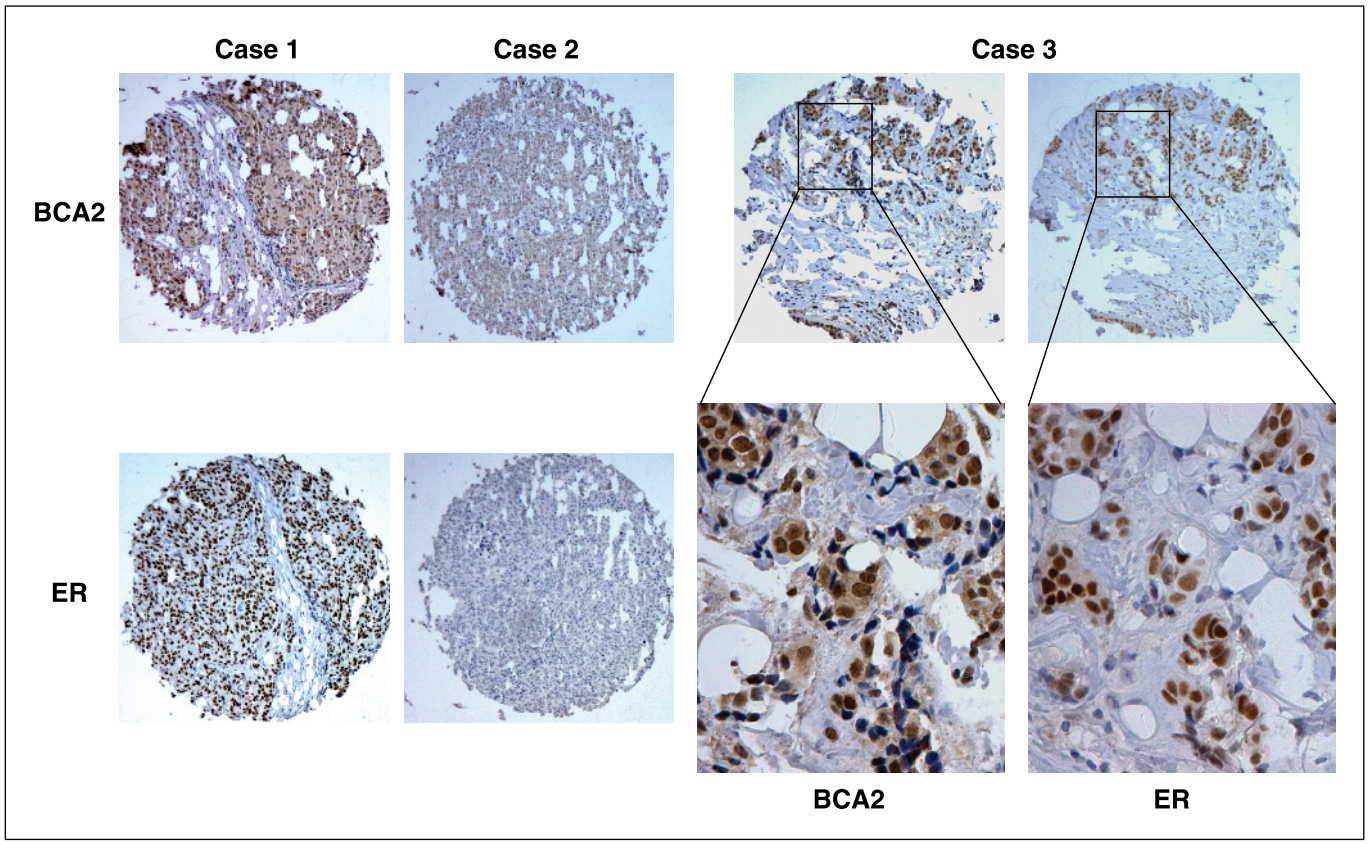

Figure 7. Comparison of three representative invasive breast cancer cases from the HBBCC tissue microarray. Consecutive tissue microarray sections were stained for ER and BCA2 as indicated and viewed at 10× magnification. Case 3 (*bottom*) shows ×40 magnification of the indicated areas of the ×10 micrographs revealing coexpression of ER and BCA2 in the nuclei of positive cells. Of the 945 invasive HBBCC cases, 67% were positive for both ER and BCA2 (Table 1).

of late endosomes/lysosomes affecting EGF degradation in mouse cells (13). These data are consistent with our observation that overexpression of the BCA2 E3 ligase increases growth, whereas its down-regulation by siRNA reduces growth and breast cancer cell invasion (Fig. 9). We confirmed the interaction of human Rab7 with human BCA2 at the level of endogenous protein in human breast cancer cells (data not shown). Thus, cytoplasmic BCA2, along with Rab7, may modulate the turnover of growth factors and cell surface

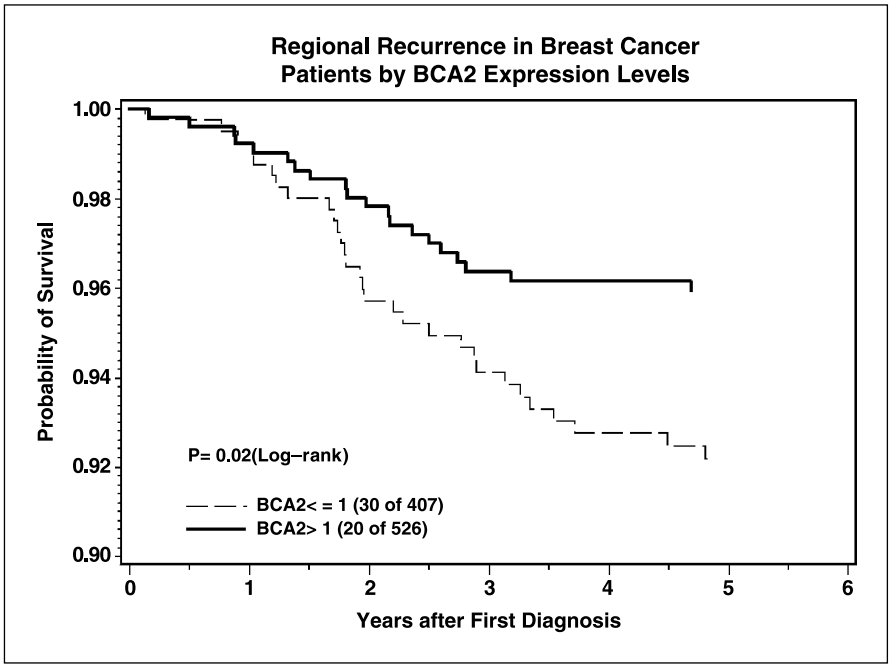

Figure 8. Kaplan-Meier curves for regional recurrence in patients with invasive breast cancer. The estimated probability of survival is compared for a patient group with BCA2 ≤ 1 and BCA2 > 1. Patients with BCA2 > 1 had a significant survival benefit of regional recurrence 5 years after first diagnosis (P = 0.02 log-rank for time from diagnosis to recurrence; compare with Table 2).

molecules important to breast cancer by affecting the biogenesis and function of lysosomes. Based on the observed altered BCA2 expression in breast cancers and its likely function in vesicle trafficking, it is of interest to consider the therapeutic potential of controlling BCA2-Rab–regulated pathways in breast cancer through pharmacologic intervention, e.g., by using zinc ejector compounds.

On the basis of RNA expression analysis by Northern and high-density tissue microarrays, we showed that BCA2 is overexpressed in invasive breast cancer compared with normal tissues and other tumor types. These data indicate that BCA2 is a tumor-associated protein. Prostate carcinomas seem to have similar expression pattern as breast cancers as seen at the RNA level and by detection of protein expression in nuclei and cytoplasm of prostate tumor tissues in a multitumor array (Fig. 5; data not shown). Thus, BCA2 might play a role in hormone-dependent cancers.

The analysis of BCA2 expression in a large cohort of 945 invasive breast cancers showed a significant correlation of its levels with ER status. Moderate to strong BCA2 expression levels (immunohistochemical score > 1) were associated with positivity for ER (P = 0.004; Table 1). ER-positive invasive breast cancers in general have a better prognosis than ER-negative tumors and are less aggressive (21). Our analysis of BCA2 expression and variables of survival and recurrence showed high nuclear BCA2 levels to be somewhat protective for regional recurrence (P = 0.05). These breast cancers were also less likely to present with lymph node metastasis (P = 0.02), but no effect on mortality was seen. Whereas BCA2 expression is associated with more favorable prognostic factors and ER status, it does not seem to correlate with survival in invasive breast cancers (Table 3). We found that overexpression of BCA2 was a favorable factor in breast cancer in relation with occurrence of lymph node metastases and regional recurrence. Another prominent example of a RING E3 ligase associated with cancer is MDM2. Its overexpression is predictive for a poor outcome in sarcomas, gliomas, and acute lymphocytic leukemia; however, it is a marker of favorable prognosis in melanoma, non–small cell lung cancers, and ER-α–positive breast cancers (29–32).

The chromosome 1q21-31 region has been shown to have a high frequency of allelic loss in breast carcinomas (12). However, an increase in 1q copy number is also a frequent finding in breast tumors by CGH and has been shown in 55% of primary invasive breast cancers (11, 12). Moreover, in patient cohorts with gain of 1q, this event is correlated with positive estrogen and progesterone receptor status and higher survival rate compared with patients with other aberrations (11). Patients with higher BCA2 protein

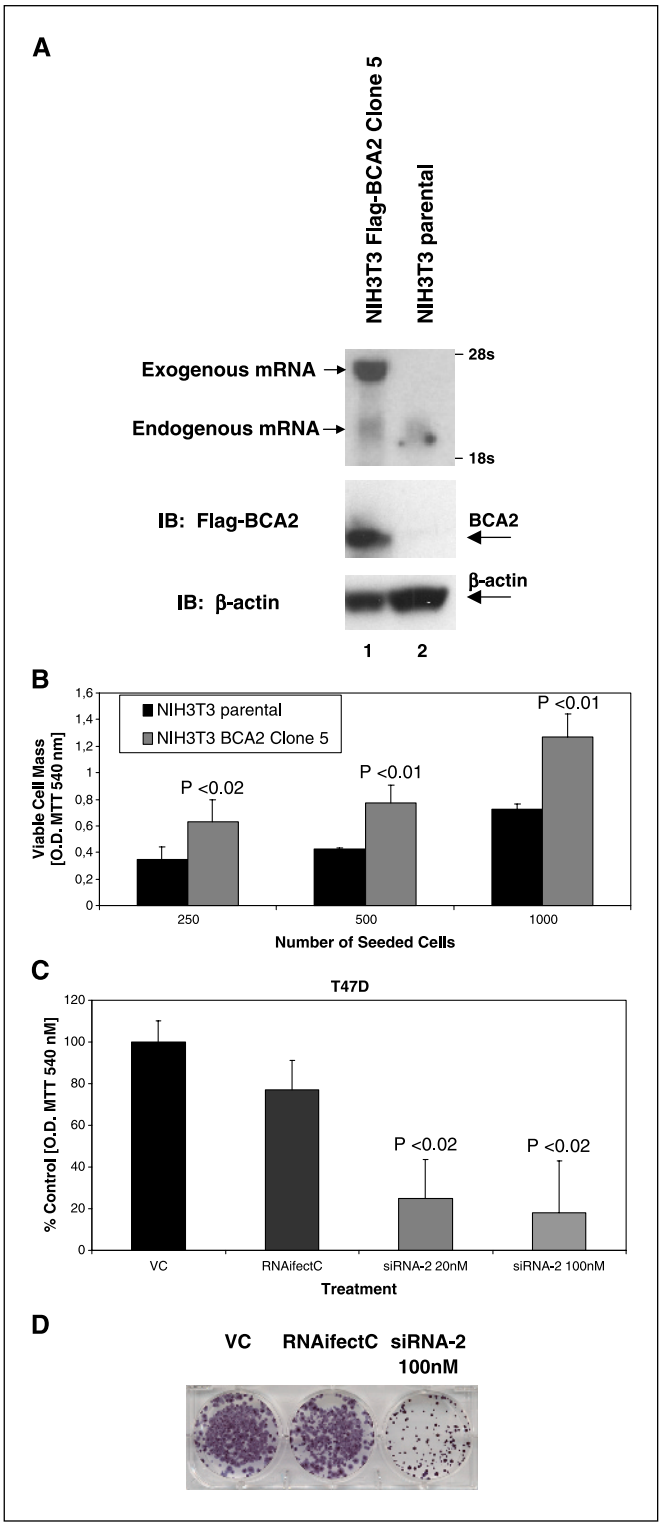

Figure 9. Effects of BCA2 on cell growth. *A,* Northern blot (*top*), anti-BCA2 immunoblot (*middle*), and antiactin immunoblot (*bottom*) of NIH3T3 cells stably transfected with human WT FLAG-BCA2 (clone 5, *lane 1*) and the parental NIH3T3 cells (*lane 2*). *B,* comparison of growth of parental NIH3T3 cells and the NIH3T3 BCA2 clone 5 cells at different seeding densities in a 6-day MTT proliferation assay. The growth differences between parental and BCA2 clone 5 cells were statistically significant with Student's t test P values of <0.02 and <0.01, respectively. *O.D.*, absorbance. *C,* comparison of growth of the breast cancer cell line T47D in a 6-day MTT proliferation assay after treatment with vehicle control siRNA suspension buffer, RNAiFect lipofection reagent control (*RNAifectC*), or with the BCA2 siRNA duplex 2 (*siRNA-2*) that also showed the most BCA2 inhibition in Fig. 5*E*. The vehicle control was set as 100%. Data are representative of three independent experiments. The vehicle control was set as 100% (absorbance 1.57 ± SD 0.16). The differences in growth between BCA2 siRNA duplex 2 treatment and controls were significantly different (P < 0.02, Student's t test). *D,* effect of BCA2 siRNA duplex 2 on the motility of MCF-7 cells through Transwell inserts (8 μm pores, Costar, Cambridge, MA). BCA2 siRNA duplex 2 (100 nmol/L) significantly decreased MCF-7 invasion (P < 0.001). Shown are representative wells of MCF-7 cells, which were able to migrate from the Transwell membrane into the bottom of these wells and attach. Vital cells were stained with MTT and photographed. Subsequently, formazan was extracted with DMSO and quantified by spectrophotometry as described in Materials and Methods. If control cell growth is set as 100% (SD ± 4.2), MCF-7 cells treated with BCA2 siRNA duplex 2 show a relative reduction in motility and invasion of 30% (SD ± 0.2), P < 0.001. Data are representative of three independent experiments.

levels may reflect this category of breast cancers as we found that 56% of invasive breast cancers overexpress BCA2 and that its protein levels correlated with ER-positive status.

Future studies are needed to clarify whether BCA2 and ER expression are coregulated and whether a causal link between ER status and BCA2 expression can be established; thus, BCA2 might provide an alternative target for the treatment of hormone-refractory breast tumors.

Acknowledgments

Received 6/15/2005; revised 9/1/2005; accepted 9/7/2005.

Grant support: Canadian Institutes of Health Research-University Industry Program, Canadian Breast Cancer Research Alliance, and Canadian Foundation for Innovation.

The costs of publication of this article were defrayed in part by the payment of page charges. This article must therefore be hereby marked *advertisement* in accordance with 18 U.S.C. Section 1734 solely to indicate this fact.

We thank Ellen Rawlinson for her efforts in organizing the Henrietta Banting Database, Xu Guo and Michael Wong for excellent technical assistance.

References

1. Glickman MH, Ciechanover A. The ubiquitin-proteasome proteolytic pathway: destruction for the sake of construction. Physiol Rev 2002;82:373–428.
2. Joazeiro CA, Weissman AM. RING finger proteins: mediators of ubiquitin ligase activity. Cell 2000;102:549–52.
3. Kosarev P, Mayer KF, Hardtke CS. Evaluation and classification of RING-finger domains encoded by the *Arabidopsis* genome. Genome Biol 2002;3:RESEARCH0016.
4. Pray TR, Parlati F, Huang J, et al. Cell cycle regulatory E3 ubiquitin ligases as anticancer targets. Drug Resist Updat 2002;5:249–58.
5. Burger AM, Seth AK. The ubiquitin-mediated protein degradation pathway in cancer: therapeutic implications. Eur J Cancer 2004;40:2217–29.
6. Burger AM, Salesiotis A, Panayiotakis A, Li H, Seth A. Identification of differentially expressed genes in breast cancer. Int J Oncol 1996;8:395–400.
7. Burger A, Li H, Zhang XK, et al. Breast cancer genome anatomy: correlation of morphological changes in breast carcinomas with expression of the novel gene product Di12. Oncogene 1998;16:327–33.
8. Burger AM, Beatty B, Seth A. Function and regulation of novel breast cancer associated genes. J Cancer Res Clin Oncol 1999;125:S15–6.
9. Burger AM, Zhang X, Seth A. Detection of novel genes that are up-regulated (Di12) or down-regulated (T1A12) with disease progression in breast cancer. Eur J Cancer Prev 1998;7:S29–35.
10. Seth A. Breast cancer associated genes and uses thereof. WO 02/0875707 A2, WIPO;2002.
11. Rennstam K, Ahlstedt-Soini M, Baldetorp B, et al. Patterns of chromosomal imbalances defines subgroups of breast cancer with distinct clinical features and prognosis. A study of 305 tumors by comparative genomic hybridization. Cancer Res 2003;63:8861–8.
12. Bieche I, Champeme MH, Lidereau R. Loss and gain of distinct regions of chromosome 1q in primary breast cancer. Clin Cancer Res 1995;1:123–7.
13. Mizuno K, Kitamura A, Sasaki T. Rabring7, a novel Rab7 target protein with a RING finger motif. Mol Biol Cell 2003;14:3741–52.
14. Subramaniam V, Lubovitz J, Li H-X, Burger A, Kitching R, Seth A. The RING-H2 protein RNF11 is overexpressed in breast cancer and is a target of Smurf2 E3 ligase. Br J Cancer 2003;I89:1538–44.
15. Yang Y, Fang S, Jensen JP, Weissman AM, Ashwell JD. Ubiquitin protein ligase activity of IAPs and their degradation in proteasomes in response to apoptotic stimuli. Science 2000;288:874–7.
16. Rice WG, Baker DC, Schaeffer CA, et al. Inhibition of multiple phases of human immunodeficiency virus type 1 replication by a dithiane compound that attacks the conserved zinc fingers of retroviral nucleocapsid proteins. Antimicrob Agents Chemother 1997;41:419–26.
17. Nash T, Rice WG. Efficacies of zinc-finger-active drugs against *Giardia lamblia*. Antimicrob Agents Chemother 1998;42:1488–92.
18. Shian SG, Kao YR, Wu FY, Wu CW. Inhibition of invasion and angiogenesis by zinc-chelating agent disulfiram. Mol Pharmacol 2003;64:1076–84.
19. Alley MC, Scudiero DA, Monks A, et al. Feasibility of drug screening with panels of human tumor cell lines using a microculture tetrazolium assay. Cancer Res 1988;48:589–601.
20. Landberg G, Ostlund H, Nielsen NH, Emdin S, Burger AM, Seth A. Downregulation of the potential suppressor gene IGFBP-rP1 in human breast cancer is associated with inactivation of the retinoblastoma protein, cyclin E overexpresson, and increased proliferation in estrogen receptor negative tumors. Oncogene 2001;20:3497–505.
21. Rampaul RS, Pinder SE, Elston CW, Ellis IO. Prognostic and predictive factors in primary breast cancer and their role in patient management: the Nottingham Breast Team. Eur J Surg Oncol 2001;27:229–38.
22. Kallioniemi OP, Wagner U, Kononen J, Sauter G. Tissue microarray technology for high-throughput molecular profiling of cancer. Hum Mol Genet 2001;10:657–62.
23. Lai Z, Yang T, Kim YB, et al. Differentiation of Hdm2-mediated p53 ubiquitination and Hdm2 autoubiquitination activity by small molecular weight inhibitors. Proc Natl Acad Sci U S A 2002;99:14734–9.
24. Chen A, Kleiman FE, Manley JL, Ouchi T, Pan ZQ. Autoubiquitination of the BRCA1*BARD1 RING ubiquitin ligase. J Biol Chem 2002;277:22085–92.
25. Arihiro K, Oda H, Kaneko M, Inai K. Cytokines facilitate chemotactic motility of breast carcinoma cells. Breast Cancer 2000;7:221–30.
26. Prest SJ, Rees RC, Murdoch C, et al. Chemokines induce the cellular migration of MCF-7 human breast carcinoma cells: subpopulations of tumour cells display positive and negative chemotaxis and differential *in vivo* growth potentials. Clin Exp Metastasis 1999;17:389–96.
27. Murphy LC, Dotzlaw H, Wong MS, et al. Epidermal growth factor: receptor and ligand expression in human breast cancer. Semin Cancer Biol 1990;1:305–15.
28. Murphy LJ, Sutherland RL, Stead B, Murphy LC, Lazarus L. Progestin regulation of epidermal growth factor receptor in human mammary carcinoma cells. Cancer Res 1986;46:728–34.
29. Higashiyama M, Doi O, Kodama K, et al. MDM2 gene amplification and expression in non-small-cell lung cancer: immunohistochemical expression of its protein is a favourable prognostic marker in patients without p53 protein accumulation. Br J Cancer 1997;75:1302–8.
30. Hori M, Shimazaki J, Inagawa S, Itabashi M. Overexpression of MDM2 oncoprotein correlates with possession of estrogen receptor α and lack of MDM2 mRNA splice variants in human breast cancer. Breast Cancer Res Treat 2002;71:77–83.
31. Onel K, Cordon-Cardo C. MDM2 and prognosis. Mol Cancer Res 2004;2:1–8.
32. Polsky D, Melzer K, Hazan C, et al. HDM2 protein overexpression and prognosis in primary malignant melanoma. J Natl Cancer Inst 2002;94:1803–6.